Design optimization of InGaAsP/InP heterostructures of high-power laser diodes emitting at a wavelength of 1.55 μm

© A.E. Rizaev, A.A. Podoskin, I.V. Shushkanov, V.A. Kapitonov, I.S. Shashkin, L.S. Vavilova, S.O. Slipchenko, N.A. Pikhtin

Ioffe Institute,
194021 St. Petersburg, Russia

E-mail: rizartem@mail.ioffe.ru

Received April 22, 2025
Revised May 5, 2025
Accepted June 3, 2025

The study aims to optimize the design of semiconductor laser heterostructures based on InGaAsP/InP, emitting in the eye-safe wavelength range of 1.55 μm in pulsed mode. The research was conducted using a developed two-dimensional laser diode model that accounts for drift-diffusion carrier transport in the direction perpendicular to the heterostructure layers and the inhomogeneous photons distribution along the resonator axis. For model laser diodes with an emitting aperture width of 100 μm, the main loss mechanisms were studied, as well as their effect on the output optical power at a pulse pump current of 150 A. The study involved multiparametric optimization, taking into account the influence of the bandgap and waveguide thickness, as well as the position of the active region within the waveguide layer. A strong dependence of the optimal waveguide thickness on its bandgap, as well as the optimal bandgap providing a balance between the main power limiting mechanisms, was established. It is shown that, regardless of other parameters, the location of the active region near the *p*-emitter is preferable.

Keywords: Semiconductor laser, leakage current, free carrier absorption, drift-diffusion transport, laser diode.

DOI: 10.61011/SC.2025.03.61562.7867

1. Introduction

InGaAsP/InP-based laser diodes operating at a wavelength of 1.55 μm are key elements of fiber-optic communication due to minimal losses in quartz fibers at this wavelength [1,2]. Also, their active use in rangefinders and LIDAR systems, where high pulse power and safety for the eyes are required, necessitates the need to increase the efficiency of such devices [3]. Currently, a number of theoretical papers have been published on the analysis and optimization of heterostructure design in order to increase the optical output power. For instance, various mechanisms of laser power loss on a GaAs substrate were studied in Ref. [4], and their contribution to saturation of the light-current characteristic was estimated. An analysis of internal losses was conducted in Ref. [5] based on a semi-analytical approach and a design of a heterostructure with a heavily doped *n*-waveguide and a strongly asymmetric active region was proposed to reduce them. At the same time, it is clear that the choice of optimal parameters of the laser heterostructure should be based on research within the framework of multiparametric optimization. To achieve these goals, it is necessary to study the influence of heterostructural parameters on the mechanisms limiting the optical power and to reduce their impact. Previous study [6] was devoted to the analysis of the mechanisms of saturation of the light-current characteristic in InGaAsP/InP-based lasers, where two main mechanisms were identified — free carrier absorption internal loss (fca) in the waveguide and electron leakage in *p*-emitter, which has a significant effect in these materials due to the low energy barrier at the waveguide/emitter interface. Taking into account the established factors limiting the optical power of the laser, it becomes necessary to change the design of the heterostructure in order to reduce their influence on the power characteristics of the radiation. This paper studies an approach aimed both at reducing the leakage current by changing the height of the waveguide/emitter barrier, and at reducing internal losses by changing the parameters of the waveguide and the position of the active region. Using numerical modeling, the influence of these parameters on the optical power and the main loss mechanisms is investigated, and the heterostructure is optimized to find parameters that provide the highest optical power of lasers operating in the pulsed mode.

2. Model description

The calculation of the electro-optical characteristics of the lasers under study was performed using a two-dimensional model of a laser diode described in Refs. [7,8]. The applied model takes into account the drift-diffusion carriers transport in the layers of the heterostructure, the inhomogeneous distribution of photons along the axis of the resonator, Shockley-Read-Hall recombination, Auger recombination and radiative recombination are taken into account in all layers of the simulated heterostructure. The pulsed mode of operation of lasers is considered in the framework of the work, which makes it possible to neglect thermal effects.

Material parameters of the heterostructure layers

		Active area	Waveguide			Emitters	Sources
			type 1	type 2	type 3		
E_g	Bandgap, eV	0.8	1.02	1.08	1.14	1.34	[9]
N_c	Effective density of states in the conduction band, cm^{-3}	$2.4 \cdot 10^{17}$	$3.7 \cdot 10^{17}$	$4.1 \cdot 10^{17}$	$4.5 \cdot 10^{17}$	$5.7 \cdot 10^{17}$	[9]
N_v	Effective density of states in the valence band, cm^{-3}	$7.6 \cdot 10^{18}$	$9.1 \cdot 10^{18}$	$9.6 \cdot 10^{18}$	10^{19}	$1.1 \cdot 10^{19}$	[9]
μ_n	Electron mobility, $cm^2/(V \cdot s)$	3500	3500	3500	3500	1500	[5,9]
μ_p	Hole mobility $cm^2/(V \cdot s)$	85	85	85	85	50	[5,9]
$\tau_{n,p}$	Shockley–Read–Hall lifetime of electrons and holes, s	$10 \cdot 10^{-9}$					
B	Radiative recombination coefficient, cm^3/s	$1.1 \cdot 10^{-10}$					[10]
$C_{n,p}$	Auger recombination coefficients, cm^6/s	$1 \cdot 10^{-29}$	$7 \cdot 10^{-29}$	$7 \cdot 10^{-29}$	$7 \cdot 10^{-29}$	$9 \cdot 10^{-31}$	[10]
n	Refractive index	3.53	3.345	3.31	3.27	3.163	[11]
σ_n	Free-carrier absorption cross section for electrons, cm^2	$5 \cdot 10^{-19}$					[12]
σ_p	Free-carrier absorption cross section for holes, cm^2	$4 \cdot 10^{-17}$					[12]
$N_{a,d}$	Concentration of ionized impurities, cm^{-3}	10^{15}	10^{15}	10^{15}	10^{15}	10^{18}	
dE_c/dE_g	Band offset	0.38					[13]

An important part of the research in the framework of multiparametric optimization using numerical modeling is the choice of an algorithm. In general, the optical output power of semiconductor lasers depends on the amplitude of the pumping current and is determined by the capabilities of available generators, as well as the needs of specific laser systems. Currently, generators are available that provide pulses with a duration of tens of nanoseconds and an amplitude of hundreds of amperes, therefore, to demonstrate the developed approach, a fixed value of the pumping current amplitude of 150 A was used for optimization in the presented work. The proposed multiparametric optimization involves investigating the influence of key parameters of the laser heterostructure based on the InGaAsP/InP system of materials: waveguide thickness, waveguide bandgap, and the position of the active region. The selected parameters determine the main radiation characteristics required in applied tasks (optical power, mode composition, beam quality), and are also available for variation in technological processes, which makes them an important object of study before production. Therefore, for clarity, optimization is carried out within the framework of three types of InGaAsP/InP-based heterostructures with a wavelength of 1.55 nm, differing in the bandgap of the waveguide. The heterostructures consist of high-alloy InP emitters with a layer thickness of 1.5 μm, an InGaAsP waveguide with E_g equal to 1.02 (type 1), 1.08 (type 2) and 1.14 eV (type 3), and an active region consisting of one an InGaAsP quantum well with $E_g = 0.8$ eV thickness of 20 nm. For each type of heterostructure, the thickness of the waveguide and the distance from the active region to the p-emitter varied during operation within 0.1–1 and 0–0.4 μm, respectively. The material parameters of the heterostructure layers used in numerical modeling are given in the following table.

The active layer gain parameters are selected according to previous paper [6]. As part of the current study, a basic 2 mm long laser crystal with reflection coefficients of 0.99 and 0.05 mirrors and a radiation aperture of 100 μm is being considered.

3. Discussion of the results

For all types of structures, two-dimensional optical power distributions were obtained depending on the waveguide thickness W and the shift of the active region to the p-emitter D (D — distance from the active region up to the boundary p-emitter/waveguide) (Figures 1–3, a), as well as two-dimensional distributions of the main losses limiting the output optical power of the leakage current and free carrier absorption internal loss (Figures 1–3, b, c) at a pulsed pump current of 150 A. It should be noted that regions with radiation generation at nonzero transverse modes are excluded from consideration. Such regions are typical for a wide multimode waveguide with an active region strongly shifted to the p-emitter. As it was shown

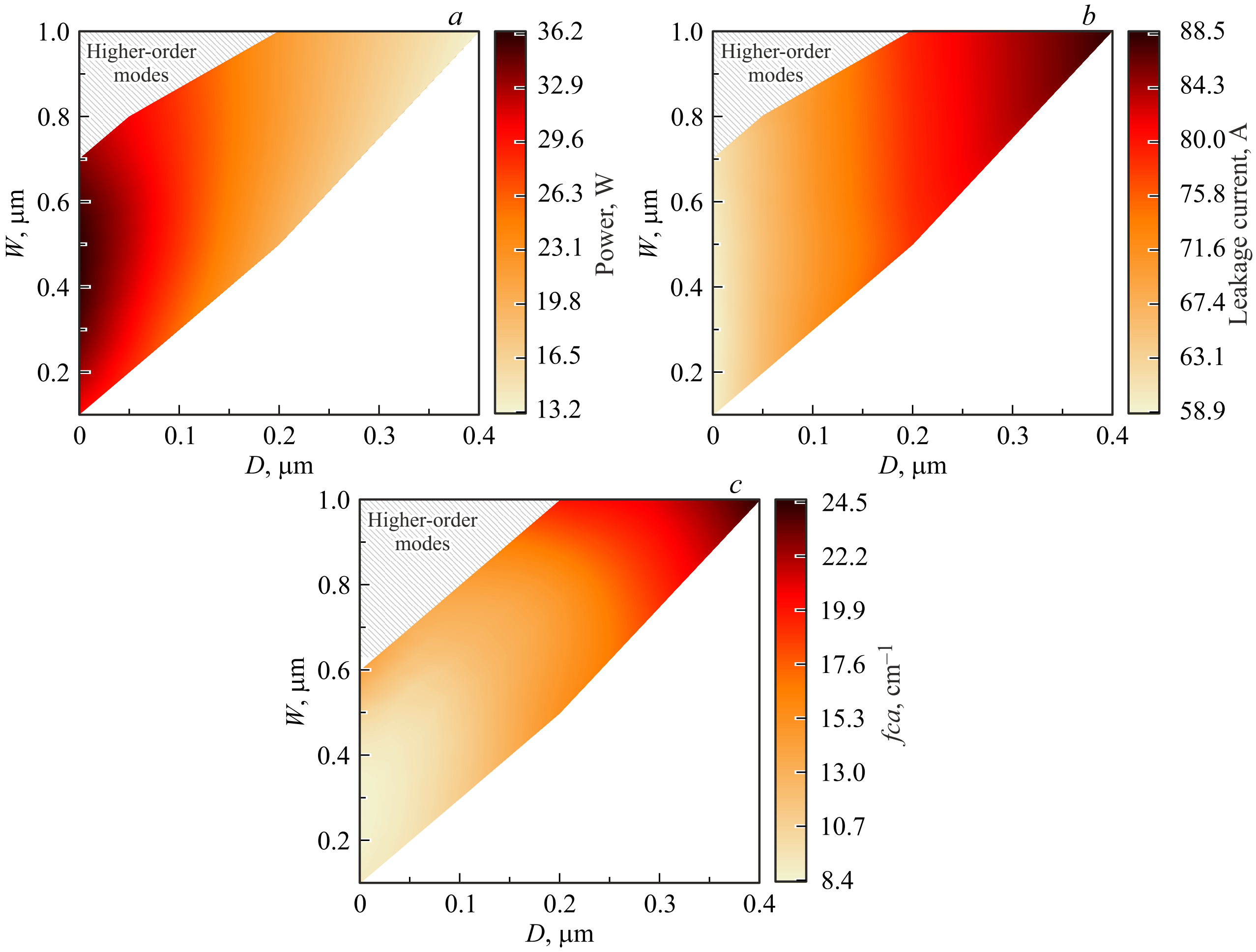

Figure 1. Two-dimensional distributions of optical power (a), leakage current (b), free carrier absorption internal loss (c) depending on waveguide thickness W and the distance from the active region to p-the emitter D in a structure of type 1 ($E_g = 1.02\,\mathrm{eV}$) at a current of 150 A. The dash indicates the area with radiation generation at nonzero modes.

earlier in Ref. [14], the possibility of selecting higher-order modes and maintaining threshold generation conditions only for the fundamental mode is possible due to a larger optical confinement factor in the active region of the fundamental mode compared to higher-order modes. When implementing the simplest design of an active region and waveguides with symmetrical emitters, this condition is difficult to fulfill in the region adjacent to the waveguide-emitter boundary due to a sharp decrease in the proportion of the zero-mode field and an increase in the proportion of the higher-order mode field. This effect increases as the E_g of the waveguide decreases, which is reflected in the expansion of the radiation region at nonzero modes, which is due to the higher contrast of the refractive indices of the structure and, consequently, the strong localization of nonzero modes in the waveguide. Also, cases close to the symmetrical location of the active region and its shift towards the n-emitter were not considered. As shown in Ref. [6], such positions of the active region lead to an increase in the effects of carrier accumulation in the waveguide and, as a result, an increase in internal optical loss and a decrease in optical output power.

Regardless of the waveguide bandgap, the highest optical power in each of the considered types of structures is achieved with the maximum shift of the active region to the p-emitter. This area is characterized by both minimal free carrier absorption loss and low leakage current (Figures 1–3). Regardless of the waveguide bandgap, the graphs shown (Figures $1-3, a$) show that there is a significant decrease in optical power as the active region moves away from the p-emitter, which is consistent with an increase in current leaks (Figures $1-3, b$). At the same time, the change in leakage current is insignificant when the thickness of the waveguide varies, i. e., the optical power achieved when the waveguide thickness W changes is attributable to a change in free carrier absorption internal loss. It should be noted that with the transition from a wide-band waveguide to a narrow-band waveguide, the region of the highest optical power shifts towards narrow waveguides (Figures $1-3, a$). The obtained dependences demonstrate that the highest optical power of 36.6W is provided by

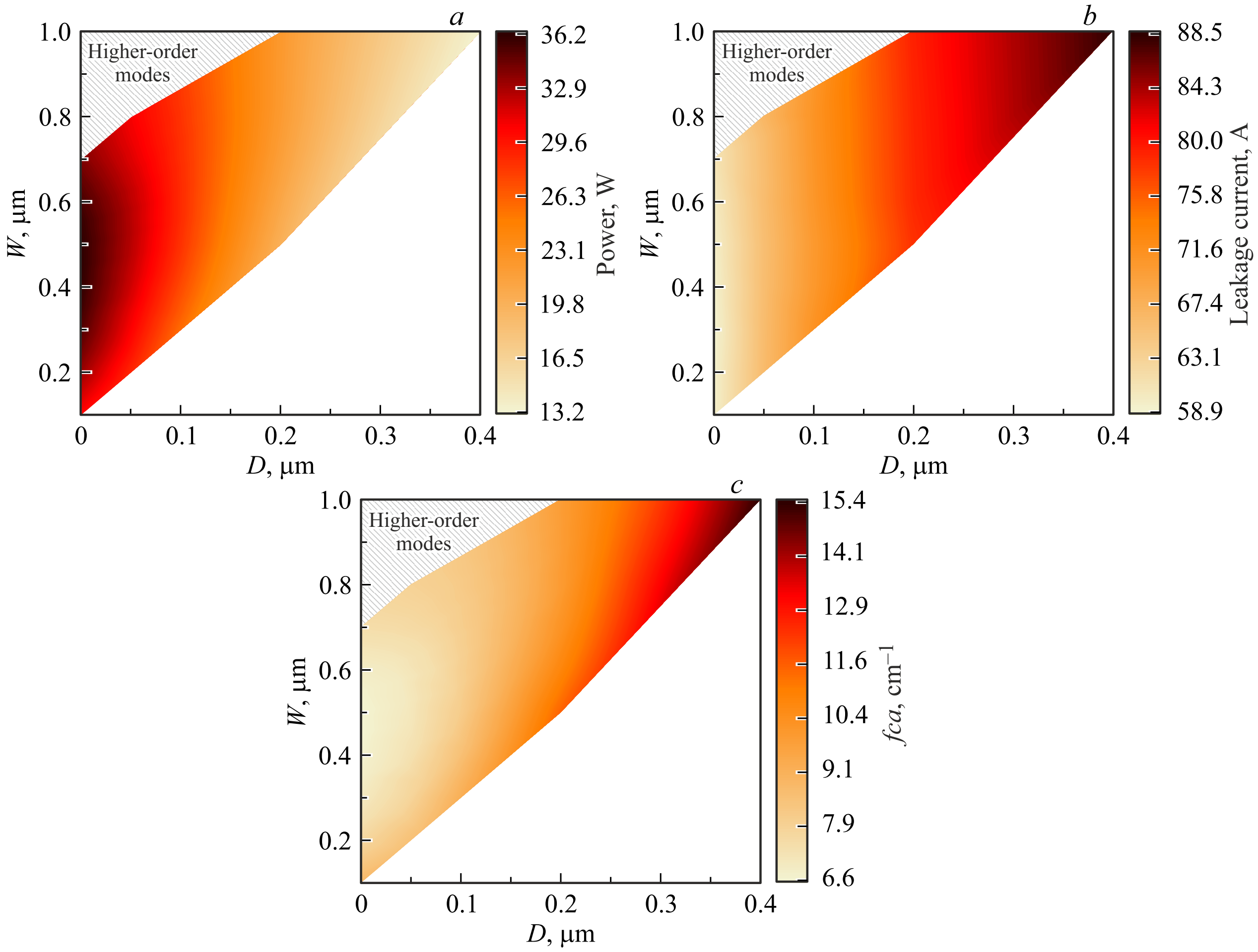

Figure 2. Two-dimensional distributions of optical power (a), leakage current (b), free carrier absorption internal loss (c) depending on waveguide thickness W and the distance from the active region to p- the emitter D in a structure of type 2 ($E_g = 1.08$ eV) at a current of 150 A. The dash indicates the area with radiation generation at nonzero modes.

a 1 type heterostructure with a narrow-band waveguide ($E_g = 1.02$ eV) with a thickness of 0.3 μm and an active region adjacent to p-emitter.

To explain the dependences obtained, using the example of a structure of type 1 with a narrow-band waveguide ($E_g = 1.02$ eV) for the point of maximum optical power, slices were constructed demonstrating the dependence of power, leakage current, and loss fca on D at a fixed $W = 0.3\,\mu$m (Figure 4) and from W at a fixed $D = 5$ nm (Figure 5). Let us consider the reason for the localization of the values of the heterostructure design parameter D, corresponding to the location of the active region near the p-emitter and providing the highest peak power. Injection of carriers from highly doped emitters with their subsequent transport in waveguide layers by the drift-diffusion mechanism leads to the accumulation of excess concentration, which is partially compensated by carriers of the opposite sign. At the same time, the higher the current density, the higher the concentration of excess carriers. The condition of a high rate of recombination in the active region, which is supported by the process of stimulated recombination and the requirement to maintain concentration in accordance with the current threshold condition, forms a „triangular" profile of the distribution of excess carrier concentrations with a maximum at the waveguide/emitter interface and a minimum at the active region. Since the holes have noticeably lower mobility, the concentration of excess holes on the side of p-emitter turns out to be noticeably higher than the concentration of excess electrons on the side of n-emitter. This fact provides an advantage of heterostructure designs in which there is a strong shift of the active region towards the p-emitter, which is associated with a significant decrease in the concentration of excess holes in part of the waveguide layer from the active region to the p-emitter and, as a result, a decrease in free carrier absorption internal loss in this part of the waveguide. In addition, a lower concentration of excess carriers near the p-emitter also reduces the leakage current, which, together with a decrease of loss fca, results in a significant gain in optical power (Figure 4).

A change in the thickness of the waveguide has little effect on the leakage current for heterostructure designs

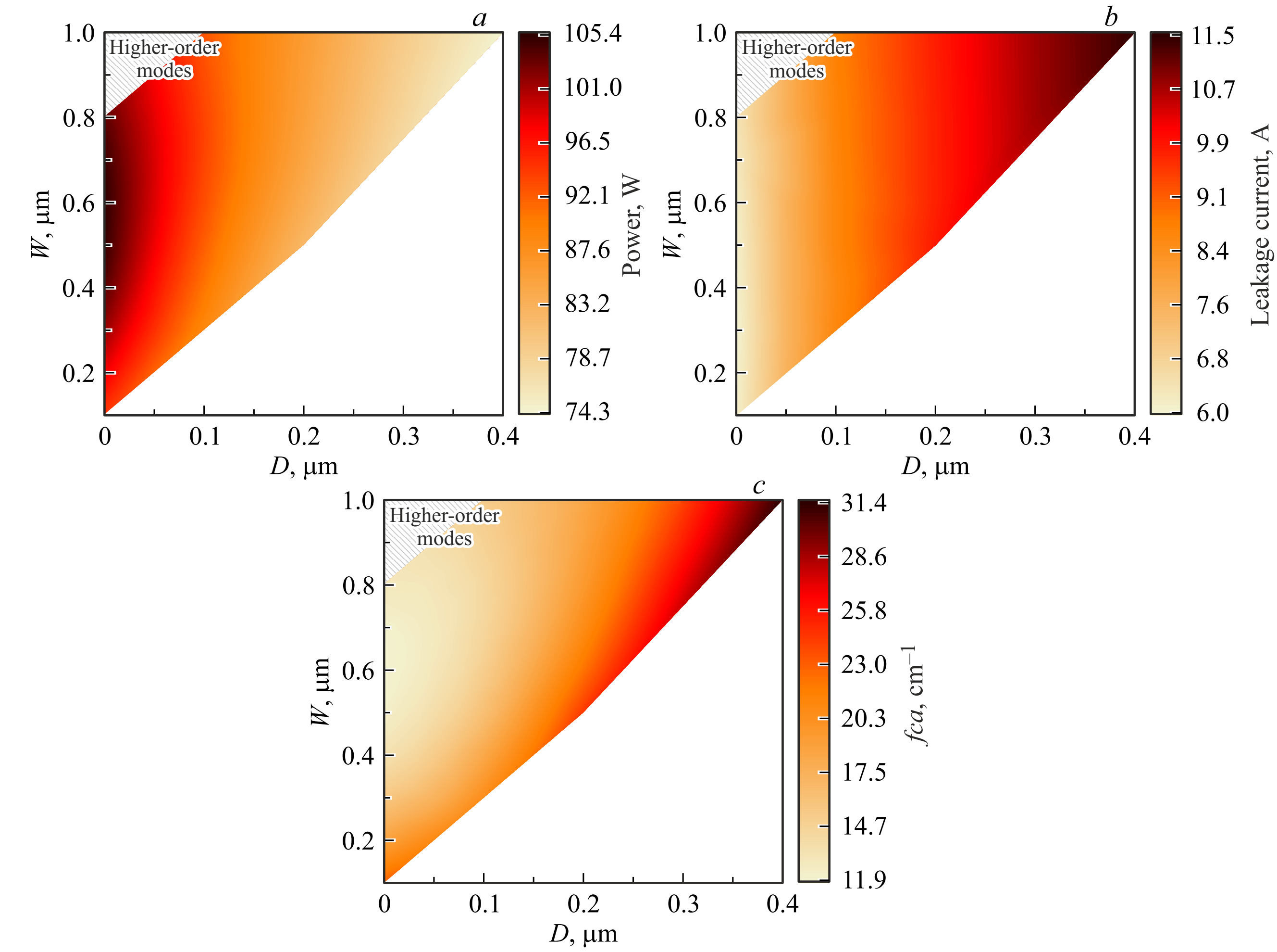

Figure 3. Two-dimensional distributions of optical power (a), leakage current (b), free carrier absorption internal loss (c) depending on waveguide thickness W and the distance from the active region to p-the emitter in a structure of type 3 ($E_g = 1.14$ eV) at a current of 150 A. The dash indicates the area with radiation generation at nonzero modes.

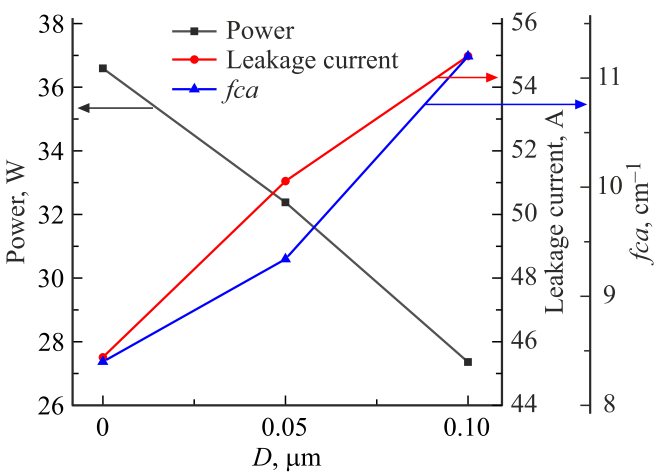

Figure 4. Dependence of optical power, leakage current, and free carrier absorption internal loss on the distance of the active region to p-emitter at a waveguide thickness of 0.3 μm in a structure of type 1 ($E_g = 1.02$,eV) at a pumping current of 150 A.

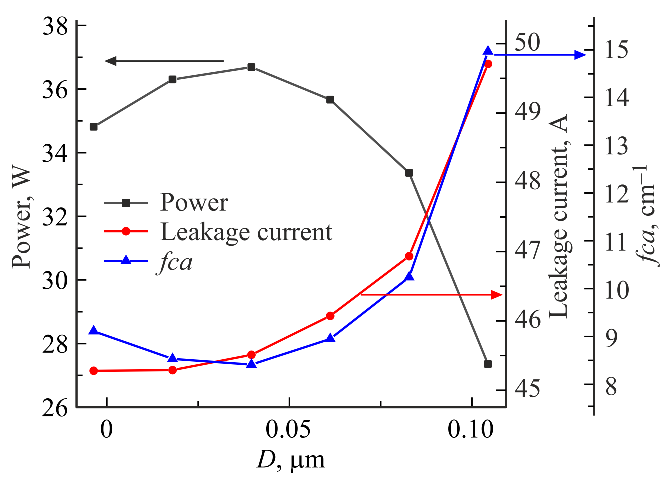

Figure 5. Dependence of optical power, leakage current and free carrier absorption internal loss on waveguide thickness in a structure of type 1 ($E_g = 1.02$ eV) at $D = 5$ nm at a pumping current of 150 A.

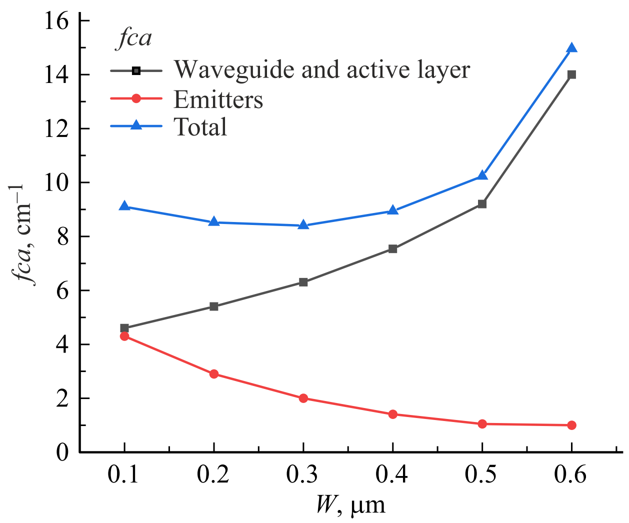

Figure 6. Free carrier absorption loss occurring on different layers of a structure of type 1 with an active region adjacent to *p*-emitter. Pumping current — 150 A.

in which D is minimal, which is associated with a low concentration of excess main carriers (holes) as the main cause of electron leakage through the heterobarrier (Figure 5). Therefore, the maximum optical power is achieved with a waveguide thickness that minimizes internal losses associated free carrier absorbtion. The greatest losses are observed in a wide waveguide, which is due to the strong localization of the mode in this layer at a high concentration of carriers. As the waveguide narrows, the localization of the mode decreases, which reduces losses in the waveguide, but increases losses in the emitters due to the greater overlap of the mode with these regions. At the same time, the different dynamics of changes in losses in the waveguide and emitters leads to the optimal thickness of the waveguide, ensuring minimal total losses (Figure 6).

Let us consider in more detail the effect of the waveguide bandgap on the studied parameters. As the bandgap of the waveguide increases (E_g), the contrast of the refractive indices of the heterostructure layers decreases, which worsens the localization of the mode, leading to an increase in losses in the emitters. As a result, the optimal thickness of the waveguide shifts to higher values (Figure 7). However, the leakage current is the key factor determining the optical power in case of varying of E_g of the waveguide. As the E_g increases, the energy barrier for carriers at the waveguide/emitter interface decreases, which critically increases the leakage of electrons into the *p*-emitter. The above dependencies also clearly demonstrate the small effect of the waveguide thickness W on the leakage current, which was discussed above. It should be noted that in structures with a small bandgap of the waveguide ($E_g = 1.08$ and 1.02 eV), similar optical power values are observed, but the loss mechanisms contributing to optical power saturation are markedly different. A situation with the highest possible barrier is realized at the waveguide/*p*-emitter heterointerface in a structure of type 1 with a narrow-band waveguide layer. As a result, the estimated leakage current has a minimum value of 45 A. Increasing the bandgap of the

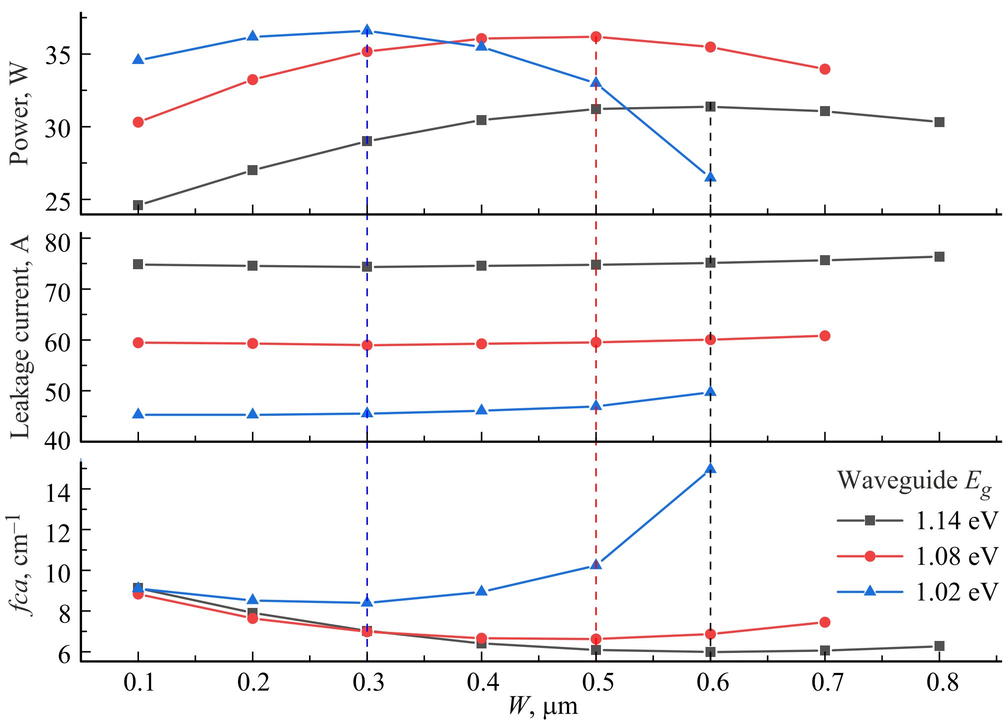

Figure 7. Dependence of optical power, leakage current, and free carrier absorption loss on waveguide thickness for 3 types of structures with different E_g of the waveguide and active region adjacent to *p*-emitter. Pumping current — 150 A.

waveguide to 1.08 eV in the structure of type 2 leads to an increase in leakage current to 60 A. On the other hand, an increase in the bandgap of the waveguide leads to a weakening of the waveguide properties and a decrease in the optical confinement factor of the fundamental mode in the waveguide. As a result, the optical loss of the type 2 structure for structures with expanded waveguides become noticeably lower than in the type 1 structure with a stronger waveguide. Thus, the bandgap has a noticeable effect on both the internal optical loss and the leakage current. As a result of the optimization, a change in the main mechanism of optical power saturation is observed with a decrease of the E_g of the waveguide from 1.08 to 1.02 eV.

Proceeding to the selection of the optimal parameters of the heterostructure, it is preferable to focus on a narrow-band structure of type 1 with a waveguide thickness of $W = 0.3\,\mu$m and an active region adjacent to the *p*-emitter to obtain the highest optical power. A further decrease in the bandgap of the waveguide is impractical due to the rapid increase in internal loss, which, due to the reduced leakage current, become the main mechanism for limiting optical power.

4. Conclusion

The effect of InGaAsP/InP-based heterostructure parameters (bandgap, waveguide thickness, and active region position) on the power of the laser diode and its losses was studied in this paper, and an optimal heterostructure design was proposed to achieve the highest optical power. The primary results showed that it is necessary to place the active region at a minimum distance from the *p*-emitter for reducing the effect of leakage current and increase the efficiency of laser diodes. Minimal internal losses associated with free carrier absorption are achieved with an optimal waveguide thickness, which provides a balance between losses in the emitter and waveguide layers of the heterostructure. At the same time, the optimal thickness of the waveguide is determined by the degree of localization of the transverse mode and, accordingly, strongly depends on the waveguide bandgap, which emphasizes the need for numerical calculations for materials of heterostructures dictated by various tasks.

The best optical power at a high pulsed pump current of 150 A was calculated for a structure with a narrow-band waveguide with a waveguide thickness of $W = 0.3\,\mu$m and an active region adjacent to the *p*-emitter, and amounted to 36.6 W. However, optimizing the structure, which uses a wider-band waveguide, allows obtaining a maximum power of 36.2 W, which is not significantly less. In this case, the choice of heterostructure design should be based on the requirements for specific practical applications. For example, the use of a structure of type 2 with a wider-band waveguide and a slight difference in power may be overridden by the possibility of using wider waveguides to improve beam quality, with smaller divergence angles, which expands the range of practical applications of a laser diode, including telecommunications and fiber-optic systems.

The technological process of manufacturing InGaAsP/InP-based heterostructures with $1.55\,\mu$m radiation has been developed over the past decades and the laser diodes produced are highly reliable. However, there is an alternative AlInGaAs/InP material system in which higher optical power can be achieved, but due to the presence of aluminum and its sensitivity to oxidation, it requires more attention to ensure reliability. Therefore, a promising area of research is the further optimization of the characteristics of lasers based on aluminum-free materials through an integrated approach to the design of a laser diode, including both the design of the heterostructure and the parameters of the laser crystal.

Funding

The work was carried out with the support of the Russian Science Foundation 22-79-10159.

Conflict of interest

The authors declare that they have no conflict of interest.

References

[1] E. Agrell, M. Karlsson, A.R. Chraplyvy, D.J. Richardson, P.M. Krummrich, P. Winzer, K. Roberts, J.K. Fischer, S.J. Savory, B.J. Eggleton, M. Secondini, F.R. Kschischang, A. Lord, J. Prat, I. Tomkos, J.E. Bowers, S. Srinivasan, M. Brandt-Pearce, Gisin. J. Optics, **18** (6), 063002 (2016).
[2] G.P. Agrawal. *Fiber-Optic Communication Systems* (John Wiley & Sons, 2012).
[3] S. Royo, M. Ballesta-Garcia. Appl. Sci., **9** (19), 4093 (2019).
[4] J. Piprek. Optical Quant. Electron., **51** (2), 60 (2019).
[5] B.S. Ryvkin, E.A. Avrutin, and J.T. Kostamovaara. Semicond. Sci. Technol., **32** (12), 125008 (2017).
[6] A.E. Rizaev, A.A. Podoskin, I.V. Shushkanov, V.A. Kryuchkov, S.O. Slipchenko, N.A. Pihtin. Kvant. elektron., **55** (3), 141 (2025). (in Russian).
[7] S.O. Slipchenko, O.S. Soboleva, V.S. Golovin, N.A. Pikhtin. Bull. Lebedev Physics Institute, **50** (5), 535 (2023).
[8] S.O. Slipchenko, V.S. Golovin, O.S. Soboleva, I.A. Lamkin and N.A. Pihtin. Kvant. elektron., **52** (4), 343 (2022). (in Russian).
[9] Y.A. Goldberg, N.M. Schmidt. *Handbook series on semiconductor parameters*, v. **2**, 1−36 (1999).
[10] L.A. Coldren, S.W. Corzine, M.L. Mashanovitch. *Diode Lasers and Photonic Integrated Circuits* (John Wiley & Sons, 2012).
[11] S. Adachi. *Optical Properties of Crystalline and Amorphous Semiconductors: Materials and Fundamental Principles* (Springer Science & Business Media, 2012).
[12] B.S. Ryvkin, E.A. Avrutin, J.T. Kostamovaara. Semicond. Sci. Technol., **35** (8), 085008 (2020).
[13] S. Adachi. *Properties of Semiconductor Alloys: Group-IV, III-V and II-VI Semiconductors* (John Wiley & Sons, 2009).
[14] S.O. Slipchenko, A.D. Bondarev, D.A. Vinokurov, D.N. Nikolaev, N.V. Fetisova, Z.N. Sokolova, N.A. Pikhtin, I.S. Tarasov. Semiconductors, **43** (43), 112 (2009).

Translated by A.Akhtyamov